

Calorimetric investigations of $(\text{NaCN})_{1-x}(\text{KCN})_x$ glasses

B. Mertz, J. F. Berret,* R. Böhmer,[†] and A. Loidl

Institut für Physik, Universität Mainz, D-6500 Mainz, Federal Republic of Germany

M. Meissner and W. Knaak

Hahn-Meitner Institut, D-1000 Berlin, Federal Republic of Germany

(Received 19 March 1990)

Results of specific-heat investigations in the glassy state of $(\text{NaCN})_{1-x}(\text{KCN})_x$ mixed crystals are presented, utilizing time-resolved and standard quasiadiabatic specific-heat techniques. Crystals with concentrations $x=0.19, 0.59,$ and 0.85 were investigated, which exhibit frozen-in orientational disorder. At low temperatures ($T \lesssim 1$ K) the typical glasslike anomalies such as a logarithmic time dependence and a linear variation with temperature were detected. The existence of an excess contribution, which in glassy materials is usually termed a T^3 excess heat capacity, could not be determined unambiguously. However, extra contributions to the specific heat were observed around 1 K.

I. INTRODUCTION

Alkali-halide alkali-cyanide mixed crystals belong to a new class of disordered materials which exhibit a collective freezing transition or reorienting moments devoid of long-range order. These orientational glasses are model systems of the amorphous state of condensed matter.¹ In the pure alkali cyanides the CN^- molecules interact via an effective exchange coupling that is mediated by lattice strains. This bilinear rotation-translation coupling drives a ferroelastic phase transition.² At lower temperatures the electric dipolar interaction forces establish long-range antiferroelectric order.³ Substitution of the CN^- molecules, e.g., by Br^- or Cl^- , introduces randomness of the anisotropic interaction between the CN^- ions and gives rise to an orientational glass state below a critical concentration x_c .^{1,3} The glass state is characterized by frozen-in local shear distortions⁴ and exhibits the low-temperature thermodynamic,⁵⁻⁷ dielectric,⁸⁻¹⁰ and elastic properties¹¹ that are characteristic of amorphous systems. For example, in $(\text{KBr})_{1-x}(\text{KCN})_x$ a linear and time-dependent specific heat has been detected below 1 K.⁵ In addition, an excess contribution to the specific heat shows up in a wide concentration range.^{6,7}

At the glass transition the relaxation dynamics is similar to that observed in real glasses with the occurrence of primary (α) and secondary (β) relaxations.^{12,13} Hence, orientational glasses combine the topological order of the center-of-mass lattice with static and dynamic properties of amorphous systems. Further interest in the cyanide glasses has been stimulated by the theoretical work of Sethna and co-workers,¹⁴ who calculated the low-temperature specific heat using a phenomenological model. According to this theory the linear term of the specific heat is understood as being due to 180° tunneling flips of the CN^- molecules. The excess specific heat was thought to arise from CN^- librational excitations coupled to the lattice. The model parameters entering Sethna's theory, e.g., the energy barriers, their distribution widths, and the attempt frequencies determine the

secondary relaxation processes at higher temperatures and, hence, can be determined by dielectric spectroscopy.^{7,14,15}

The theoretical treatment of cyanide glasses was analogous to that of spin glasses, which focused on the random bond disorder and disregarded the random-field effects completely. This approach was used in the early works of Fischer and Klein¹⁶ and Michel and Rowe,¹⁷ and later on in the framework of infinite-range mean-field models.¹⁸⁻²¹ Monte Carlo simulations have been performed on orientational glasses with nearest-neighbor interactions by Carmesin and Binder.²² Recently, K. H. Michel described the relaxation phenomena in the cyanide glasses within the framework of a random-field model.²³ Static random strains, which are generated by substitutional atoms of different sizes, couple linearly to the orientations of the CN^- ions. Later on, the theory was extended by including a nonergodic instability.²⁴

In $(\text{NaCN})_{1-x}(\text{KCN})_x$, static random strains are implanted by the volume difference of the Na^+ and K^+ ions, which are distributed statistically on the cationic sublattice, whereas the CN^- sublattice remains undiluted. Thus, in a first approximation, it seems plausible that this system is dominated by random fields and is ideal to test the role played by random strains.

A schematic phase diagram of solid solutions of potassium and sodium cyanides determined from optical transmission experiments²⁵ and from neutron diffraction²⁷ is shown in Fig. 1. Two critical concentrations at $x_{c1} \approx 0.16$ and $x_{c2} \approx 0.90$ appear in this system. At intermediate concentrations the system is dominated by strong random strains. Neutron-scattering results revealed that near $x \approx 0.5$ the freezing in of the CN^- quadrupoles is dominated by the strong random fields and is almost a single-ion phenomenon.²⁸ Close to x_{c2} the freezing transition is highly cooperative and strong deviations from a pure random field behavior were detected.²⁸

The aim of the present work was to study the low-temperature specific heat in $(\text{NaCN})_{1-x}(\text{KCN})_x$ in the glassy regime with special attention to the following questions

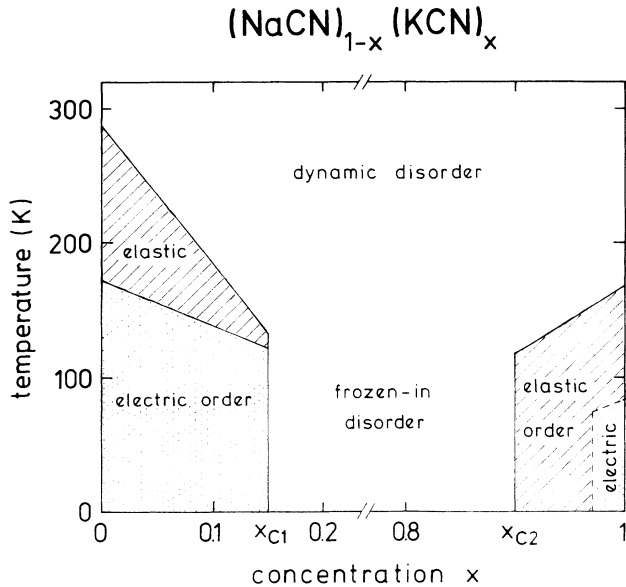


FIG. 1. Schematic phase diagram of $(\text{NaCN})_{1-x}(\text{KCN})_x$ composed after a neutron-scattering work of Schröder *et al.* (Ref. 26). The hatched areas indicate the elastically ordered regions, while the dotted ones represent those exhibiting an anti-ferroelectric order (Ref. 26). Between the two critical concentrations $x_{c1}=0.16$ and $x_{c2}=0.90$ an orientational glass state is observed at low temperatures (Refs. 25, 26, and 28).

(i) Does the low-temperature specific heat reflect glassy behavior?

(ii) Is there any difference in the low-temperature specific heat of the random field system $(\text{NaCN})_{1-x}(\text{KCN})_x$ compared with $(\text{KBr})_{1-x}(\text{KCN})_x$, which possibly is a random bond system and which has been studied in full detail?⁵⁻⁷

(iii) Do the low-temperature properties reveal a signature of the freezing process (single-ion freezing at intermediate concentrations and a cooperative freezing transition near x_{c2})?

II. EXPERIMENT AND RESULTS

$(\text{NaCN})_{1-x}(\text{KCN})_x$ mixed crystals with concentrations $x=0.19$, 0.59 , and 0.85 were delivered from the Crystal Growth Laboratory of the University of Utah and from J. Albers at the Physics Department of the Universität des Saarlandes. The actual concentrations of the mixed crystals have been determined using atomic absorption spectrophotometry²⁹ and from the room-temperature lattice constants.³⁰

The samples were cleaved from the mother crystals and prepared similarly to those reported in Ref. 5. The surfaces were roughened with sandpaper in order to provide a uniform sample heating. The thin samples of thickness $d \approx 0.5$ mm were rectangularly shaped ($\approx 8 \times 4$ mm²) and thermally anchored to three thin copper rods. With this arrangement a very short internal thermalization time ($t_{in} \leq 100$ μ s) and a much longer external sample-to-bath time constant ($t_{ex} \geq 100$ ms) was achieved. Short-time heat pulses ($t_p \approx 1$ μ s) applied by an evaporat-

ed gold film heater combined with time-resolved carbon film thermometry allowed an observation of internal temperature relaxation processes within the quasiadiabatic time window 0.1 ms $\lesssim t \lesssim 0.1$ s. The sample temperature-time profiles $\Delta T(T_0, t)$ were analyzed and transformed into a time-dependent specific heat $C_p(T_0 + \Delta T, t)$. It has been demonstrated in different types of crystals that results using time-resolved specific-heat measurements are in good agreement with long-time data as obtained by standard quasiadiabatic $C_p(T)$ techniques.³¹

In addition, an analysis of the short-time temperature profiles (heat pulse propagating diffusively through the sample) does provide the temperature dependence of the thermal diffusivity $D(T, t_{\text{expt}})$ (at $t_{\text{expt}} \leq 0.1$ ms) and the nonstationary thermal conductivity $K(T, t_{\text{expt}})$ below 1 K.³²

Long-time specific-heat measurements for $T \gtrsim 2.5$ K were carried out in a standard quasiadiabatic calorimeter by applying Joule heat to samples having a mass of approximately 1.5 g. The temperature versus time profiles were measured with a germanium ($2 \leq T \leq 50$ K) or a platinum ($10 \leq T \leq 100$ K) resistance thermometer. From these profiles the specific heat of the samples was automatically calculated using a computerized data acquisition system.³³

In Fig. 2 specific-heat results of the three $(\text{NaCN})_{1-x}(\text{KCN})_x$ mixed crystals ($x=0.19$, 0.59 , and 0.85) are depicted for temperatures $T \leq 1$ K and for two measuring times $t_0=0.1$ ms and 0.1 s. Deviations from the Debye-like T^3 behavior of insulating crystals are clearly apparent. Below $T \approx 300$ mK, Fig. 2 shows an almost linear variation of the specific heat C_p with temperature. This indicates a nearly constant distribution of low-energy excitations. In addition a strong dependence of C_p on the experimental time scale is observed. At a

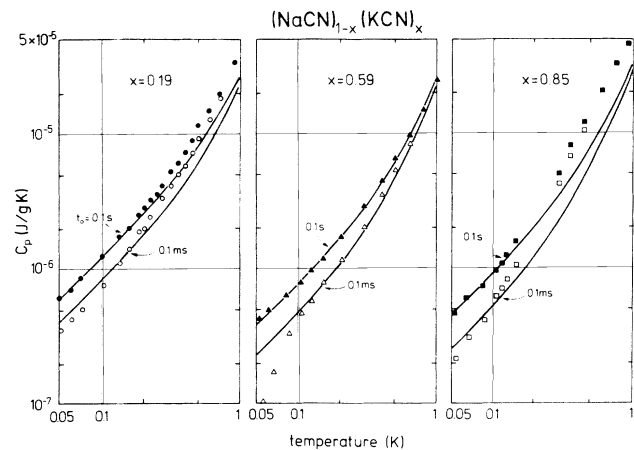


FIG. 2. Temperature dependence of the measured specific heat $C_p(T, t)$ for three single crystals of $(\text{NaCN})_{1-x}(\text{KCN})_x$ with $x=0.19$, 0.59 , and 0.85 at measuring times $t=0.1$ s and 0.1 ms. The solid lines are calculated with Eq. (3), using C_3 , $C_1^{t=1s}$, and \bar{P} as listed in Table I taking into account data up to $T \approx 6$ K.

base temperature $T_0 = 100$ mK an increase of the measuring time t_0 by three decades enhances the specific heat by nearly a factor of 2. For the $(\text{NaCN})_{0.41}(\text{KCN})_{0.59}$ sample a stronger dependence of $T \lesssim 100$ mK has been observed. The solid lines in Fig. 2 represent the calculated specific heat using Eq. (3). The parameters C_3 , α , C_1 , and \bar{P} were determined by fits to the experimental data shown in Figs. 3 and 4, respectively.

The long-time specific heat is shown in Fig. 3 plotted as C_p/T^3 versus T for temperatures $50 \text{ mK} \leq T \leq 100 \text{ K}$. For $(\text{NaCN})_{0.41}(\text{KCN})_{0.59}$ a set of data was obtained by the two different measuring techniques which overlap at $T \approx 2.5 \text{ K}$. Unfortunately, the low-temperature data for $x = 0.85$ and 0.19 have been taken only for $T \lesssim 1 \text{ K}$. In the representation C_p/T^3 versus T a conventional insulating crystal would exhibit a plateau for $T/\Theta_D \lesssim 0.07$, which indicates normal Debye-like behavior. With increasing T the C_p/T^3 data then continuously would decrease. In contrast, Fig. 3 reveals the following features.

(i) The linear variation of the specific heat at lowest temperatures is strongly pronounced for all samples investigated,

(ii) A well-defined plateau exists for $2 \lesssim T \lesssim 6 \text{ K}$. An excess specific-heat bump which usually appears in canonical glasses between 3 and 15 K is absent. However, the plateau regime is considerably enhanced compared to pure KCN (Ref. 7) and NaCN (Ref. 33) as indicated by solid lines,

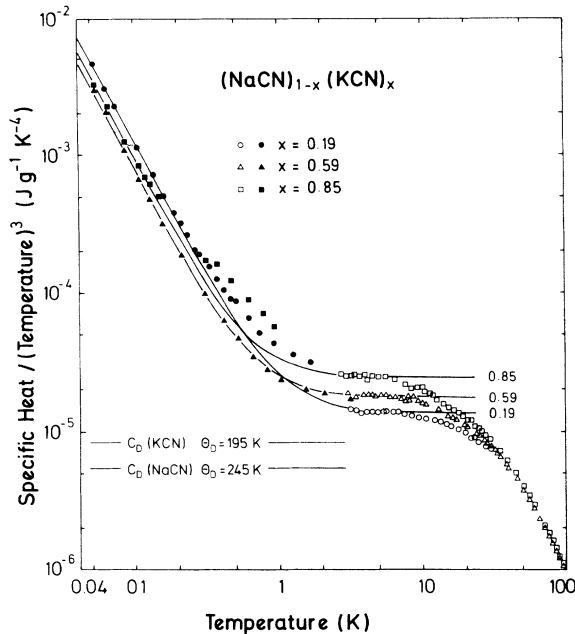


FIG. 3. Complete sets of long-time specific-heat data of $(\text{NaCN})_{1-x}(\text{KCN})_x$. Open symbols show data obtained with an adiabatic calorimeter; solid symbols mark “long-time” data ($t_{\text{expt}} = 0.1 \text{ s}$) measured using time-resolved thermometry. The solid lines are best fits according to Eq. (3) and parameters given in Table I. For $(\text{NaCN})_{0.15}(\text{KCN})_{0.85}$ and $(\text{NaCN})_{0.81}(\text{KCN})_{0.19}$ extra contributions are observed around 1 K (see also Fig. 6). Indicated are the Debye contributions at lowest temperatures for the pure ends of the mixed system (Refs. 7 and 33).

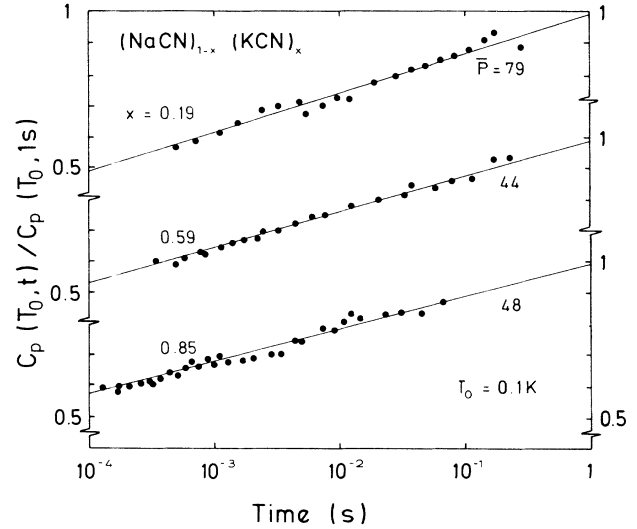


FIG. 4. Normalized time-dependent specific heat vs time of the three $(\text{NaCN})_{1-x}(\text{KCN})_x$ crystals at $T_0 = 0.1 \text{ K}$. $C_p(T_0, t)/C_p(T_0, t = 1 \text{ s})$ varies logarithmically with measuring time. The spectral densities $\bar{P}(x)$ (in 10^{44} J/m^3) of two-level systems are determined from the slopes of the straight lines fitted to the data points according to Eq. (4).

(iii) Extra contributions appear near 1 K for $(\text{NaCN})_{0.81}(\text{KCN})_{0.19}$ and $(\text{NaCN})_{0.15}(\text{KCN})_{0.85}$ (see also Figs. 2 and 6). Similar experimental findings were observed in Suprasil W and will be discussed later.

The low- and high-temperature specific-heat data of the crystals with $x = 0.19$ and 0.85 (both close to the critical concentrations) and $x = 0.59$ reveal that these crystals undergo no phase transitions down to the lowest temperatures.

III. ANALYSIS AND DISCUSSION

This chapter is organized as follows: (i) the low-temperature linear and time-dependent specific heat is analyzed within the framework of the standard tunneling model; (ii) the existence of glasslike excess contributions at intermediate temperatures is investigated; (iii) the observed extra modes for the $(\text{NaCN})_{1-x}(\text{KCN})_x$ samples with $x = 0.19$ and 0.85 are inspected; and (iv) a brief discussion of the thermal conductivity and diffusivity obtained from the time-dependent specific-heat results is given. The first two subsections include some remarks concerning Sethna’s model calculations, which were originally developed to explain the low- T specific-heat anomalies in $(\text{KBr})_{1-x}(\text{KCN})_x$.¹⁴

A. Linear and time-dependent specific heat

In canonical glasses the low- T specific heat ($T \lesssim 1 \text{ K}$) is well represented by a polynomial of the form³⁴

$$C_p = C_1(t_0)T^\alpha + (C_D + C_{\text{exc}})T^3. \quad (1)$$

with $\alpha \approx 1$. The first term of Eq. (1) accounts for an almost linear T variation of C_p at the lowest temperatures and includes also the logarithmic time dependence. The

“excess” specific-heat contribution is represented by C_{exc} , in addition to the normal Debye specific heat C_D of insulating crystals. Equation (1) is only a rough approximation of the low- T specific heat in glasses which is commonly used to fit the experimental results below 1 K. At higher temperatures the excess term usually results in a bump in C_p when plotted as C_p/T^3 versus T .^{6,7} The (NaCN)_{1-x}(KCN)_x samples show a different dependence (see Fig. 3). The experimental observation yields $C_p \sim T^n$, where $n \approx 1$ for $T \leq 0.3$ K and $n \approx 3$ for $2.5 \leq T \leq 6$ K and allows us to approximate the data (measured at $t_{\text{expt}} = t_0$) in a temperature range $0.05 \leq T \leq 6$ K.

The standard tunneling model (STM) developed by Anderson, Halperin, and Varma³⁵ and by Phillips³⁶ accounts for the linear temperature and the logarithmic time dependences of the low-temperature specific heat. This model assumes a constant spectral distribution $\bar{P} = P(\lambda, \Delta)$ of two-level systems (TLS) characterized by a tunneling parameter λ and an asymmetry parameter Δ . The time-dependent prefactor of the linear term of Eq. (1) within the framework of the STM is calculated by³²

$$C_1(t) = \frac{1}{12\rho} \pi^2 k_B^2 \bar{P} \ln(4t/\tau_{\text{min}}), \quad (2)$$

where ρ is the mass density and τ_{min} is the shortest TLS phonon relaxation time. Normalizing the data to a certain measuring time, e.g., $t = 1$ s, eliminates τ_{min} .⁵ Combining Eqs. (1) and (2) and using $\alpha = 1$ yields

$$C_p(T, t = 1 \text{ s}) = \left[C_1(t = 1 \text{ s}) + \frac{1}{12\rho} \pi^2 k_B^2 \bar{P} \ln \left[\frac{t}{1 \text{ s}} \right] \right] T^\alpha + C_3 T^3 \quad (3)$$

with $C_3 = C_{\text{exc}} + C_D$. Fits using Eq. (3) are shown in Figs. 2 and 3 by the solid lines.

The density of tunneling states \bar{P} can be derived from the slope of the time-dependent data $C_p(T_0, t)$ (Fig. 4) at fixed sample temperatures T_0 and normalized to the long-time specific heat:⁵

$$\frac{C_p(T_0, t)}{C_p(T_0, t = 1 \text{ s})} = 1 + \frac{\pi^2 k_B^2}{12\rho} \frac{\bar{P} T \ln(t/1 \text{ s})}{C_p(T_0, t = 1 \text{ s})}. \quad (4)$$

In the temperature range $0.05 \leq T_0 \leq 0.7$ K the time dependence for the three samples investigated was rather similar. In Fig. 4 the normalized experimental C_p data are plotted versus $\log_{10} t$ at $T_0 = 0.1$ K. The solid lines in Fig. 4 represent best fits according to Eq. (4) with the parameters \bar{P} as indicated. The fit parameters obtained by these fits are listed in Table I. The variation of \bar{P} at different temperatures is about $\pm 25\%$ (see Table I). Only at $T \lesssim 0.08$ K do the spectral densities increase up to $\bar{P} \approx 90 \cdot 10^{44} \text{ J}^{-1} \text{ m}^{-3}$. Figure 2 reveals a strong decoupling of two-level systems for $T \gtrsim 10$ mK, which is most pronounced for (NaCN)_{0.41}(KCN)_{0.59}. This may be interpreted as an enhanced density $P(E, \tau)$ of two-level systems at lower-energy splittings. It is interesting to note that in this temperature regime the logarithmic time dependence still holds. A similar behavior was reported in (KBr)_{0.50}(KCN)_{0.50} for $T < 80$ mK.⁵

As can be seen from Table I the concentration-dependent variations of the parameters C_1 and C_3 are relatively small in (NaCN)_{1-x}(KCN)_x. In addition, the spectral density $\bar{P}(x)$ depends only slightly on x (Table I). Thus the low-temperature properties ($T \leq 1$ K) of (NaCN)_{1-x}(KCN)_x do not reflect the different characters of the freezing processes that were detected experimentally in neutron-scattering studies.²⁸

For the orientational glass (KBr)_{1-x}(KCN)_x the low-temperature specific heat was described by a phenomenological model,¹⁴ which should also be applicable to (NaCN)_{1-x}(KCN)_x. This theory, based on the model character of the cyanide system, assumes that the linear term $C_1(t)$ originates from a 180° tunneling motion of

TABLE I. Compilation of low-temperature data of (NaCN)_{1-x}(KCN)_x (this work) and (KBr)_{1-x}(KCN)_x (Ref. 5). The mass densities ρ at low temperatures ($T \approx 4$ K) are interpolated between the pure ends assuming Vegard's law. The coefficient of the T^3 term C_3 is given by $(C_D + C_{\text{exc}})$ while $C_1(t = 1 \text{ s})$ is the coefficient of the linear T term in Eq. (1). Both quantities result from best fits of Eq. (3) to the specific heat at measuring times $t = 0.1$ s and 0.1 ms as shown in Figs. 2 and (note that C_3 is well defined by the plateau in Fig. 3). The spectral densities \bar{P} of the two-level systems as used in the standard tunneling model are determined from best fits of $C_p(T_0, t)$ data according to Eq. (2) normalized to $C_p(T_0, t = 1 \text{ s})$ (see Fig. 4). τ_{min} is the shortest TLS relaxation time which has been determined by the ratio $\rho C_1(t)/k_B^2 \bar{P}$ according to Eq. (2).

Crystal	ρ (g/cm ³)	$C_D + C_{\text{exc}}$ (10 ⁻⁵ J/g K ⁴)	$C_1^{(t=1 \text{ s})}$ (10 ⁻⁶ J/g K ²)	\bar{P} (10 ⁴⁴ /J/m ³)	τ_{min} (s)
NaCN	1.65 ^a	0.54 ^a			
(NaCN) _{0.81} (KCN) _{0.19}	1.64	1.4	13.5	60 ± 15	3 × 10 ⁻¹⁰
(NaCN) _{0.41} (KCN) _{0.59}	1.62	1.8	8.5	45 ± 10	1.5 × 10 ⁻⁸
(NaCN) _{0.15} (KCN) _{0.85}	1.61	2.5	10.5	60 ± 15	8 × 10 ⁻⁸
KCN	1.60 ^b	2.06 ^b			
(KBr) _{0.30} (KCN) _{0.70}	1.95	1.46 + 0.84	0.43	2.7	1 × 10 ⁻⁹
(KBr) _{0.50} (KCN) _{0.50}	2.18	1.73 + 0.11	0.9	9	3.5 × 10 ⁻⁶
(KBr) _{0.75} (KCN) _{0.25}	2.50	1.34 + 0.76	2.4	40	3 × 10 ⁻⁴

^aReference 33.

^bReference 5.

CN⁻ ions within the double-well potentials. The distribution of the barriers against CN⁻ reorientations is created in the quadrupolar freezing process (α relaxation) (Ref. 12) and can be determined by dielectric spectroscopy of the β relaxation, i.e., by measuring the slowing down of the electric dipoles of the CN⁻ ions in the local hindering potential.^{7,15}

(NaCN)_{1-x}(KCN)_x represents a further model system to test Sethna's predictions. For the three (NaCN)_{1-x}(KCN)_x samples, the distribution parameters (mean hindering barriers E_0 , distribution widths σ and the attempt frequencies Γ_0) were determined elsewhere.³⁹ It has been shown that the time-dependent specific-heat data below 700 mK can be parametrized within this theory.³⁹ However, the values obtained for the asymmetry Δ of the two-level systems (see Table II) turned out to be very small compared to the value of $\Delta = 340$ K for pure KCN.¹⁵ Furthermore, the asymmetry in (NaCN)_{1-x}(KCN)_x depends on the K⁺ concentration in contrast to the (KBr)_{1-x}(KCN)_x system, where a concentration-independent asymmetry parameter was assumed^{14,15} and gave a good agreement with experimental findings. The small values of Δ and the concentration dependence of Δ raised some doubts concerning the validity of Sethna's model in (NaCN)_{1-x}(KCN)_x glasses.³⁹ In addition, it is worthwhile to mention that in N₂: Ar: CO mixtures the absence of the polar CO molecules did not affect the low-temperature specific-heat anomalies.⁴²

B. Excess contribution

For all three crystals a similar plateau is observed in the C_p/T^3 versus T plot for $3 \lesssim T \lesssim 6$ K (Fig. 3). Two possible explanations seem likely: (i) a real T^3 excess term dominates in this temperature region, or (ii) the samples represent Debye solids with Debye temperatures low compared to the pure compounds. In order to solve this problem one has to evaluate the Debye contributions C_D from the Debye temperatures Θ_D . A comparison of C_D with the experimentally determined C_3 values would reveal the excess term C_{exc} . The Debye temperatures can

be determined from the low- T elastic constants by applying the harmonic series expansion method.⁴⁰ Gathering values from literature^{27,41} (see Table II) and making use of Alers's approach yields Debye temperatures as depicted in Fig. 5 by the open squares and listed in Table II. Alternatively, Θ_D can be determined directly from the specific heat by fitting the Debye integral to the specific-heat data as described earlier.⁷ Solid circles represent results as obtained from these fits. In Ref. 7 it was shown that this fitting procedure yields a reliable value of Θ_D for pure KBr. We have to admit that the strong rotation-translation coupling in the mixed cyanides may yield strong deviations from a linear phonon dispersion at low frequencies and thus introduces additional uncertainties in Θ_D . In Fig. 5 the Debye temperatures are compared to those as calculated from the plateau regions assuming a crystalline solid (open circles). The results carry relatively large error bars and do not reveal unambiguous evidence for C_{exc} terms.

C. Extra modes around 1 K

Below 1 K (Fig. 2) roughly linear specific-heat contributions are observed for all mixed crystals, which is a typical result for glasses.³⁴ However, around $T = 1$ K marked extra specific-heat contributions show up for two of the samples ($x = 0.19$ and 0.85 ; see Figs. 2, 3, and 6). Such an observation has not been made in the related (KBr)_{1-x}(KCN)_x system, nor is it known from glassy crystals in general. To our knowledge a similar finding has only been reported for Suprasil W (Refs. 37 and 38), which is a high-purity synthetic vitreous silica ($a\text{-SiO}_2$). This feature is not observed in other types of vitreous silica such as Suprasil, although Suprasil contains ≈ 1000 ppm OH⁻ impurities compared to ≤ 8 ppm OH⁻ content in Suprasil W (the halide impurity concentration is similar for both samples ≈ 100 ppm).³⁸ It has been suggested that the anomaly is of Schottky type with an energy-level splitting of some degrees Kelvin and a density of states $n_s \approx 10^{18} \text{ cm}^{-3}$.³⁸ However, the physical nature of the underlying extra modes remained unclear.³⁸

In order to provide an estimate for these extra modes

TABLE II. Averaged values of the elastic constants $c_{ij}(x, T)$ for the (NaCN)_{1-x}(KCN)_x system at low temperatures ($T \leq 20$ K) as taken from literature (Refs. 27 and 41). The c_{12} values were set equal to 1 GPa as the variation of c_{12} does not influence the Debye temperature strongly. The harmonic series expansion method (Ref. 40) was applied to calculate Θ_D^l from the c_{ij} while Θ_D^p were obtained by fits of Debye integrals to the high-temperatures ($10 \lesssim T \lesssim 30$ K) specific heat. For NaCN data from Ref. 33 were taken: $\Theta_D = 245$ K. In case of $x = 0.19$ and 0.85 the extra contributions were analyzed as Schottky-like anomalies with energy splittings E_s and number densities n_s . The asymmetries of the double-well potentials Δ were obtained from fits (Ref. 39) applying Sethna's approach (Ref. 14) for the time-dependent specific-heat term (for $x = 1$, Δ was taken from Ref. 15).

X	c_{44} (GPa)	c_{11} (GPa)	Θ_D^l (K)	Θ_D^p (K)	E_s (K)	n_s (cm ⁻³)	Δ (K)
0.19	2.58	38	189	200	3.8	7.6 10 (Ref. 18)	13.7
0.59	1.9	35.1	160	185			148
0.85	1.35	29.8	134	170	2.7	4.6 10 (Ref. 18)	30
1.00				195			340

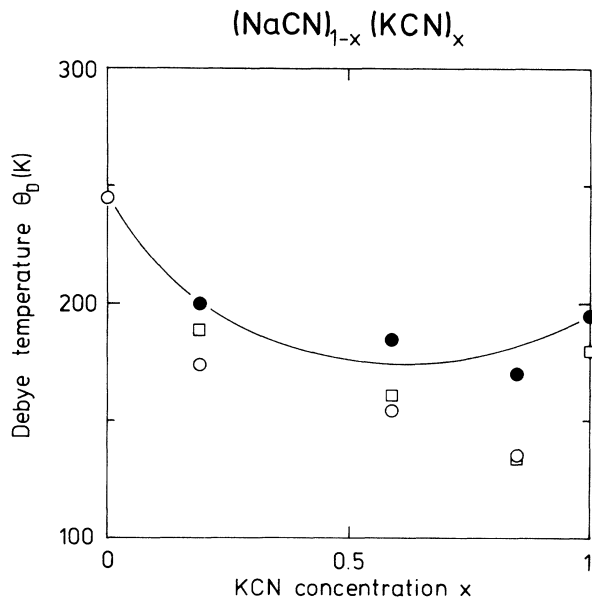


FIG. 5. Concentration dependence of the Debye-temperature Θ_D in the $(\text{NaCN})_{1-x}(\text{KCN})_x$ system as obtained by different methods: ●, from fits of the Debye integral to the high-temperature specific-heat results (for $x=1$, Θ_D^p was taken from Ref. 7); ○, obtained from the plateaus in the C/T^3 vs T plots at intermediate temperatures (see Fig. 3) using Debye's theory ($x=0$ from Ref. 33); □, averaged Θ_D values as obtained from the harmonic series expansion method (Ref. 40) using elastic constants c_{ij} at low temperatures as observed in Brillouin (Ref. 41) and neutron (Ref. 27) scattering works and from ultrasonic measurement (Ref. 27). For $x=1$, Θ_D^g was taken from Ref. 5 as determined by elastic constants.

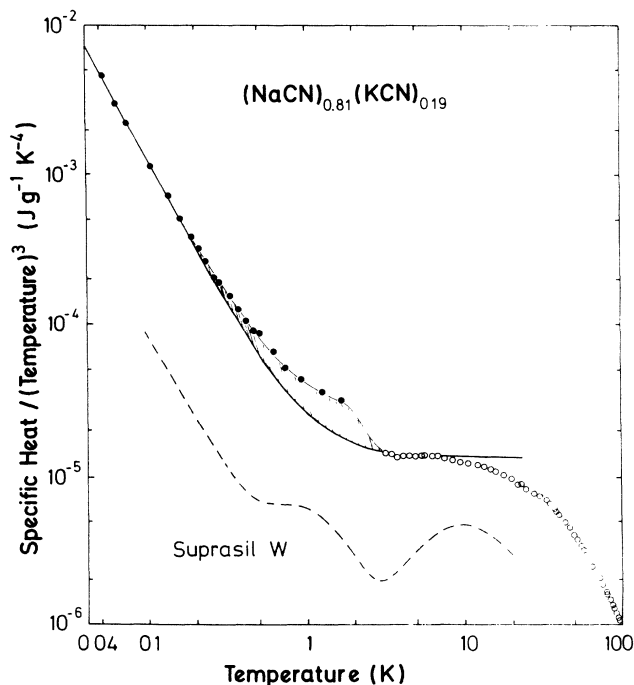


FIG. 6. Specific heat of $(\text{NaCN})_{0.81}(\text{KCN})_{0.19}$ together with that of Suprasil W (Refs. 37, 38, and 43) for comparison. The hatched area marks the occurrence of extra modes. ΔC_p estimated using Eq. (5) can be represented by a Schottky-like anomaly [Eq. (6)] with parameters as shown in Table II.

in $(\text{NaCN})_{1-x}(\text{KCN})_x$ glasses the extra specific heat ΔC_p defined by

$$\Delta C_p = C_p - [C_3 T^3 + C_1(t_0 = 1 \text{ s})T] \quad (5)$$

was analyzed in terms of a Schottky-like anomaly

$$\Delta C_p = 3AN_L k_B \frac{x^2 \exp(x)}{[\exp(x) + 1]^2} \quad (6)$$

with

$$x = E_S / T, \quad (7)$$

N_L being Avogadro's number, k_B is the Boltzmann's constant, E_S is the Schottky energy, and A is a scaling factor that gives the number of Schottky centers per volume.

Figure 6 depicts the specific heat of $(\text{NaCN})_{0.81}(\text{KCN})_{0.19}$ together with data for Suprasil W taken from literature.^{37,38,43} The Schottky parameters are listed in Table II. The obtained results for the Schottky-energy splitting E_S and the density of Schottky states n_s that follows from the scaling factor A in Eq. (6) compare well with those cited for Suprasil W. However, this similarity should not be overemphasized.

D. Thermal conductivity and diffusivity

For $(\text{NaCN})_{0.81}(\text{KCN})_{0.19}$, De Yoreo *et al.* measured the thermal conductivity $K(T)$ in a temperature range $0.07 \leq T \leq 100$ K.^{5,44} The temperature dependence and the magnitude of $K(T)$ were observed to be very similar to that of structural glasses. Below $T \approx 1$ K the thermal conductivity⁵ can be fitted to the tunneling model prediction:

$$K = AT^2 \quad (8)$$

with

$$A = \frac{2\pi k_B^3}{h^2 \bar{P} \bar{\gamma}^2} \rho v_D, \quad (9)$$

$\bar{\gamma}$ the average coupling energy for resonant interactions between TLS and phonons, and the Debye velocity v_D . Reference 5 gave no value for $\bar{\gamma}$ in the $(\text{NaCN})_{0.81}(\text{KCN})_{0.19}$ sample. Using the values $A = 3.1 \times 10^{-4}$ W/cm K³, $v_D = 1.25 \times 10^3$ m/s, and \bar{P} and ρ according to Table I for $x=0.19$, an average coupling energy $\bar{\gamma} = 0.13$ eV was calculated using Eq. (8). This value compared well with those for the related system $(\text{KBr})_{1-x}(\text{KCN})_x$ (Ref. 5) and those for structural glasses,⁴⁵ e.g., Se ($\gamma_t = 0.14$ eV), As_2S_3 ($\gamma_t = 0.17$ eV), and polystyrene ($\gamma_t = 0.13$ eV).

The thermal conductivity data of the two mixed crystals with $x=0.59$ and 0.85 have not been reported so far. Therefore, the short-time profiles from the present investigation were analyzed in terms of a thermal diffusivity $D(T, t)$ (at $t_{\text{expt}} \leq 0.1$ ms). The temperature dependence of $D(T)$ below 1 K and the subsequently calculated non-stationary thermal conductivity $K(T, t) = \rho C_p(t) D(T)$ are very similar to what is observed in glasses.^{46,47} We can state that for all three mixed crystals of $(\text{NaCN})_{1-x}(\text{KCN})_x$ the specific heat and the thermal

conductivity exhibit the typical glasslike thermal anomalies below 1 K.

E. Comparison with $(\text{KBr})_{1-x}(\text{KCN})_x$

Finally, we compare the results for $(\text{NaCN})_{1-x}(\text{KCN})_x$ with the values reported for $(\text{KBr})_{1-x}(\text{KCN})_x$ (see Table I). In the latter system low-temperature glassy properties have been observed for $x > x_c$ ($x = 0.70$) yielding small densities of state \bar{P} values.⁵ For $x < x_c$, the glassy contributions increased drastically as shown by a variation of $\bar{P} \sim (1-x)^n$ with $n \approx 3$.⁴⁷ For $x \leq 0.25$ the thermal properties exhibit increasing deviations from the standard TLS behavior. In Table I for $(\text{KBr})_{0.75}(\text{KCN})_{0.25}$ the highest $\bar{P} = 40 \times 10^{44} \text{ J}^{-1} \text{ m}^{-3}$ is comparable to those observed in the present study. In general, when compared to glasses, the spectral densities for the $(\text{NaCN})_{1-x}(\text{KCN})_x$ system are the largest observed in thermal experiments so far.

The TLS parameters for $(\text{KBr})_{1-x}(\text{KCN})_x$ vary strongly with concentration, while those for $(\text{NaCN})_{1-x}(\text{KCN})_x$ vary only slightly. We further checked the related shortest relaxation time τ_{\min} , which is related to \bar{P} via Eq. (2). For $(\text{NaCN})_{1-x}(\text{KCN})_x$ the variation of τ_{\min} is small (by a factor ≈ 250), whereas for $(\text{KBr})_{1-x}(\text{KCN})_x$ it varies by a factor of 10^5 . Calculating τ_{\min} from the ratios $\rho C_1/k_B^2 \bar{P}$ an estimate for the minimum TLS relaxation time is obtained.⁵ For $(\text{KBr})_{0.75}(\text{KCN})_{0.25}$ the shortest relaxation time $\tau_{\min} = 0.3$ ms seems to be unphysical, whereas for $(\text{KBr})_{0.30}(\text{KCN})_{0.70}$ $\tau_{\min} = 1$ ns is an acceptable value. For $(\text{NaCN})_{1-x}(\text{KCN})_x$, $\tau_{\min}(x)$ lies in the range from 0.3 to 80 ns. Obviously the substitution of the spherical K^+ ions by the smaller Na^+ ions, which increases the static random strain fields, gives rise to an increased density of TLS states compared to the density of states which result from a distortion of the KCN lattice by a substitution of CN^- ions by Br^- ions. An increasing dilution of the KCN lattice by Br^- ions increases the spectral density of low-energy states, but the distribution $P(\tau)$ becomes different from the standard TLS form.

IV. CONCLUSIONS

The calorimetric investigation of $(\text{NaCN})_{1-x}(\text{KCN})_x$ mixed crystals with $x = 0.19, 0.59,$ and 0.85 reveals features characteristic of glasses. The low-temperature specific heat varies linearly with T and shows a logarithmic time dependence over several decades. The absolute values for the linear term $C_1(t)$ and the density of two-level systems \bar{P} are much higher compared to those in $(\text{KBr})_{1-x}(\text{KCN})_x$. The \bar{P} values are the largest observed in thermal experiments on glasses so far, and five times as high compared to the canonical glass SiO_2 .

The low-temperature specific-heat anomalies, especially the parameters $C_1(t)$, \bar{P} , and C_3 do not reflect the differences which have been observed experimentally in the freezing processes.²⁸

The Debye temperatures were calculated from elastic constants c_{ij} taken from literature and compared to those as obtained by fits of the Debye integral to the specific heat. No unambiguous evidence for an excess term can be given so far.

An analysis of the low-temperature specific heat within the framework of Sethna's model yields asymmetry energies with a strong concentration dependence and with absolute values that are much smaller than those reported for $(\text{KBr})_{1-x}(\text{KCN})_x$.

The two samples close to the critical concentrations depict extra contributions to the specific heat.

ACKNOWLEDGMENTS

We thank M. Müller, R. O. Pohl, and T. Schröder for fruitful discussions, and L. Gruber for providing his Symbolic Interactive Programmable Fitter program. One of use (B.M.) thanks the Berlin group for the kind hospitality during his stay at the Hahn-Meitner Institut and the Technische Universität in Berlin while performing the measurements. This work has been partly supported by the Sonderforschungsbereich 262 and by the Material Science Research Center in Mainz. The Université de Montpellier, France is "Unité associée au Centre National de la Recherche Scientifique No. 1119."

*Permanent address: Université de Montpellier, France.

†Present address: Department of Chemistry, Arizona State University, Tempe, Arizona 85287.

¹A. Loidl, *Annu. Rev. Phys. Chem.* **40**, 29 (1989); K. Knorr, *Phys. Scr. T* **19B**, 531 (1987).

²K. H. Michel and J. Naudts, *Phys. Rev. Lett.* **39**, 212 (1977).

³F. Lüty, in *Defects in Insulating Crystals*, edited by V. M. Turkevich and K. K. Svarts (Springer-Verlag, Berlin, 1981), pp. 69–89.

⁴A. Loidl, T. Schröder, K. Knorr, R. Böhmer, B. Mertz, T. Vogt, H. Mutka, M. Müller, H. Jex, and S. Haussühl, *Z. Phys. B* **75**, 81 (1989).

⁵J. J. De Yoreo, M. Meissner, R. O. Pohl, J. M. Rowe, J. J. Rush, and S. Susman, *Phys. Rev. Lett.* **51**, 1050 (1983). J. J. De Yoreo, W. Knaak, M. Meissner, and R. O. Pohl, *Phys. Rev. B* **34**, 8828 (1986).

⁶S. K. Watson, D. G. Cahill, and R. O. Pohl, *Phys. Rev. B* **40**,

6381 (1989).

⁷B. Mertz, R. Böhmer, B. Eisele, and A. Loidl, *Z. Phys. B* **79**, 431 (1990).

⁸D. Moy, J. N. Dobbs, and A. C. Anderson, *Phys. Rev. B* **29**, 2160 (1984).

⁹M. C. Foote and B. Golding, *J. Phys.* **1**, 7751 (1989).

¹⁰G. Baier, M. V. Schickfus, and C. Enss, *Europhys. Lett.* **8**, 487 (1989).

¹¹J. F. Berret, P. Doussineau, M. Meissner, and W. Schön, *Phys. Rev. Lett.* **55**, 2013 (1985).

¹²U. G. Volkman, R. Böhmer, A. Loidl, K. Knorr, U. T. Höchli, and S. Haussühl, *Phys. Rev. Lett.* **56**, 1716 (1986).

¹³M. A. Doverspike, M. C. Wu, and M. S. Conradi, *Phys. Rev. Lett.* **56**, 2284 (1986).

¹⁴J. P. Sethna and K. S. Chow, *Phase Trans.* **5**, 317 (1985); M. Meissner, W. Knaak, J. P. Sethna, K. S. Chow, and J. J. De Yoreo, *Phys. Rev. B* **32**, 6091 (1985); J. P. Sethna, N. Y.

- Acad. Sci. **484**, 130 (1986); M. Randeria and J. P. Sethna, Phys. Rev. B **38**, 12 607 (1988); E. R. Grannan, M. Randeria, and J. P. Sethna, Phys. Rev. Lett. **60**, 1402 (1988).
- ¹⁵R. M. Ernst, L. Wu, S. R. Nagel, and S. Susman, Phys. Rev. B **38**, 6246 (1988); L. Wu, R. M. Ernst, Y. H. Jeong, S. R. Nagel, and S. Susman *ibid.* **37**, 10 444 (1988).
- ¹⁶B. Fischer and M. W. Klein, Phys. Rev. Lett. **43**, 289 (1979).
- ¹⁷K. H. Michel and J. M. Rowe, Phys. Rev. B **22**, 1417 (1980).
- ¹⁸P. Goldbart and D. Sherrington, J. Phys. C **18**, 1923 (1985).
- ¹⁹D. J. Gross, I. Kanter, and H. Sompolinsky, Phys. Rev. Lett. **55**, 304 (1985).
- ²⁰I. Kanter and H. Sompolinsky, Phys. Rev. B **33**, 2073 (1986).
- ²¹T. R. Kirkpatrick and D. Thirumalai, Phys. Rev. B **36**, 5388 (1987).
- ²²H. O. Carmesin and K. Binder, Z. Phys. B **68**, 375 (1987); H. O. Carmesin and K. Binder, Europhys. Lett. **4**, 269 (1987).
- ²³K. H. Michel, Phys. Rev. Lett. **57**, 2188 (1986); Phys. Rev. B **35**, 1405 (1987); **35**, 1414 (1987).
- ²⁴K. H. Michel, Z. Phys. B **68**, 259 (1987); C. Bostoen and K. H. Michel, *ibid.* **71**, 369 (1988).
- ²⁵F. Lüty and J. Ortiz-Lopez, Phys. Rev. Lett. **50**, 1289 (1983); J. Ortiz-Lopez, thesis, University of Utah, 1983 (unpublished).
- ²⁶T. Schröder, A. Loidl, and T. Vogt, Z. Phys. B (to be published).
- ²⁷T. Schröder, A. Loidl, T. Vogt, and V. Frank, Physica B **156&157**, 195 (1989); M. Müller, Diplomarbeit, Universität Mainz, 1989 (unpublished).
- ²⁸A. Loidl, T. Schröder, R. Böhmer, K. Knorr, J. K. Kjems, and R. Born, Phys. Rev. B **34**, 1238 (1986); T. Schröder, A. Loidl, G. J. McIntyre, and C. M. E. Zeyen, Phys. Rev. B (to be published); T. Schröder, A. Loidl, and V. Frank, in *Phonons 89*, edited by S. Hunklinger, W. Ludwig, and G. Weiss (World Scientific, Singapore, 1990), pp. 594–596.
- ²⁹M. DeLong, private communication; see also J. J. DeYoreo, thesis, Cornell University, 1985, p. 172 (unpublished).
- ³⁰T. Schröder, A. Loidl, and T. Vogt, Phys. Rev. B **39**, 6186 (1989).
- ³¹W. Knaak and M. Meissner, in *Phonon Scattering in Condensed Matter V*, edited by A. C. Anderson and J. P. Wolfe (Springer-Verlag, Berlin 1986), p. 174ff; W. Knaak, thesis, Technische Universität Berlin, 1986 (unpublished).
- ³²J. L. Black, Phys. Rev. B **17**, 2740 (1978).
- ³³B. Mertz, thesis, Universität Mainz, 1990 (unpublished).
- ³⁴R. O. Pohl, in *Amorphous Solids, Low Temperature Properties*, edited by W. A. Phillips (Springer-Verlag, Berlin, 1981), pp. 27–52.
- ³⁵P. W. Anderson, B. I. Halperin, and C. M. Varma, Philos. Mag. **25**, 1 (1972).
- ³⁶W. A. Phillips, J. Low-Temp. Phys. **7**, 351 (1972).
- ³⁷J. C. Lasjaunias, A. Ravex, M. Vandorpe, and S. Hunklinger, Solid State Commun. **17**, 1045 (1975).
- ³⁸H. v. Loehneysen and M. Platte, Z. Phys. B **36**, 113 (1979).
- ³⁹B. Mertz, Ferroelectrics (to be published); R. Böhmer, Diplomarbeit, Universität Mainz (1985), and unpublished.
- ⁴⁰G. A. Alers, in *Physical Acoustics, Vol. IIIB*, edited by P. W. Mason (Academic, New York, 1965), p. 1ff.
- ⁴¹J. F. Berret and R. Feile, Z. Phys. B (to be published).
- ⁴²C. I. Nicholls, L. N. Yadon, D. G. Haase, and M. S. Conradi, Phys. Rev. Lett. **59**, 1317 (1987).
- ⁴³M. Meissner and K. Spitzmann, Phys. Rev. Lett. **46**, 265 (1981); K. Spitzmann, thesis, Technische Universität, Berlin, 1981 (unpublished).
- ⁴⁴The concentration $x=0.25$ given in Ref. 5 for the $(\text{NaCN})_{1-x}(\text{KCN})_x$ sample was that of the melt and has to be corrected to that in the solid as $x=0.19$; see also Refs. 29 and 30.
- ⁴⁵J. F. Berret, and M. Meissner, Z. Phys. B **70**, 65 (1988). Here, γ_t is the coupling constant to transverse ultrasound waves, which contributes strongest to the averaged $\bar{\gamma}$ in a thermal conductivity experiment. The three selected “soft” glasses vary in glass transition temperature $T_g \approx 300\text{--}450$ K, transverse sound velocity $v_t \approx (1.0\text{--}1.5) \times 10^3$ m/s, and TLS spectral density $\bar{P} \approx (20\text{--}28) \times 10^{44} \text{ J}^{-1} \text{ m}^{-3}$.
- ⁴⁶J. E. Lewis, J. C. Lasjaunias, and G. Shumacher, J. Phys. (Paris) Colloq. **39**, C6-967 (1978).
- ⁴⁷J. F. Berret and M. Meissner, in Ref. 31, p. 52ff.